JOURNAL OF OPTOELECTRONICS AND ADVANCED MATERIALS Vol. 10, No. 2, February 2008, p. 264 - 268

Magnetic fluid particle sizing by coherent light scattering. Computer simulation results

D. CHICEA
Physics Department, University Lucian Blaga of Sibiu, Dr. Ion Ratiu Str. 7-9, Sibiu, 550012, Romania

Magnetic fluids are suspensions of nano to micrometer sized magnetic particles in liquids that act as scattering centers when light passes through the medium. If coherent light is incident the result of the far field interference is a "speckled" image. In a suspension the SCs have a complex movement of both sedimentation and the Brownian motion. As a result of the SCs permanent position changes the speckle image is not static but presents time fluctuations. A computer code to simulate the dynamics of the coherent light scattering on magnetic fluid was written, tested and used to calculate the far field intensity variation for nanofluids having different particle size. The results are discussed and an experimental method for fast nanoparticle size assessing is suggested.

(Received September 25, 2007; accepted February 7, 2008)

Keywords: Suspensions, Computer simulation, Image processing, Biospeckles

1. Introduction

The nanofluid notion is a relatively new notion and was first mentioned by Choi in 1995 [1] as he noticed that a small amount of nanoparticles, added in a fluid, considerably enhanced the heat transfer properties [2].

The nanoparticles have a continuous, irregular motion in nanofluids, which is the effect of several factors such as gravity, Brownian force, Archimede's force and friction force between fluid and particles. The irregular nanoparticle motion in the fluid is the cause of the remarkable enhancement of heat transfer properties of the nanofluids [3-6]. The irregular motion directly depends of the particle dimension, therefore particle velocity techniques will furnish information on the nanoparticle size.

Measuring the nanoparticle velocity resembles much measuring the velocity distribution of flow field by seeding fluids with small particles, like the particle image velocimetry, laser Doppler velocimetry and laser speckle velocimetry techniques, therefore the computer experiment presented in this work considers a speckle analysis technique [7], [8].

The seeding particles must scatter enough light to produce a good signal-to-noise ratio in order to be proper for laser particle velocimetry, therefore the diameter of the seeding particle is typically in the micrometer range. The nanoparticles though have a much smaller diameter, around 10 nanometers [9] and the intensity of the scattered light is much smaller. Results of experimental work done on coherent light scattering by nanoparticles was reported in [10-12] but they refer to processing the static far field images, not the light scattering dynamics.

In this work a program to simulate the dynamics of the light scattering by nanoparticles is described and the results of the simulation for nanoparticles with different diameters are presented.

2. The algorithm

When a medium having scattering centers randomly distributed is the target for a coherent light beam, an un-uniformly illuminated image is obtained, currently named speckled image, as a result of the interference of the wavelets scattered by the scattering centers (SC hereafter). The image changes in time as a consequence of the scattering centers complex movement of sedimentation and Brownian motion. This produces fluctuations of the image intensity in each location of the interference field. These fluctuations give the aspect of "boiling speckles" [7] [8]. In this work the objective speckle [7], respectively far field speckle [8] is considered.

The program considers coherent light having the wavelength of 632 nm to be incident on a cuvette containing the suspension. The active area of the glass cuvette (beam transversal area and light pass) are adjusted as input parameters. The far field interference pattern was calculated at a distance D apart from the simulated cuvette, which is considered to be located within the coherence region of the light source. The schematic of the computer simulation setup is presented in Fig. 1.

First the scattering centers positions were generated in the active area of the cuvette using random numbers with uniform distribution.

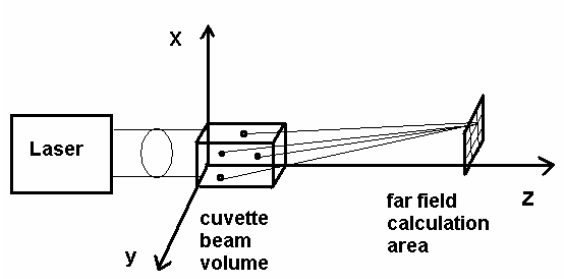

Fig. 1. The schematic of the computer simulation.

The pixel size on the simulated interference field was chosen to be the same as the pixel size of the CMOS matrix of a web camera that had the optical system removed.

Unlike in [11], the single act light scattering anisotropy on a SC was modeled using the one parameter, single scattering Henyey Greenstein phase function [13], [14] (1).

$$f(\mu)=\frac{1}{2}\frac{1-g^2}{\left(1-2\mu g+g^2\right)^{\frac{3}{2}}} \tag{1}$$

where μ=cos(θ). The anisotropy parameter, g, is currently defined as the mean cosine of the polar scattering angle θ, g=<cos(θ)>. Consequently, for light scattering strongly peaked in the forward direction, the anisotropy parameter g is close to 1 while for isotropic scattering it is zero.

The complex amplitudes of the electric field intensity scattered by each SC were added on each pixel. The electric field intensity of the interference field of a specific pixel on the screen is proportional to the integral of the f function in (1) over the cosine of the polar angle interval covered by the pixel, [μ1, μ2] and with Δφ, the azimuthal angle interval and is described by equation (2):

$$E(d,\theta,\varphi)=\frac{E_0 S_0}{d}\cdot\frac{1-g^2}{2g}\cdot \cdot\left[\left(\frac{1}{\sqrt{1+g^2-2\mu_2 g}}\right)-\left(\frac{1}{\sqrt{1+g^2-2\mu_1 g}}\right)\right]\cdot\Delta\varphi \tag{2}$$

In (2) d is the actual SC – pixel distance, E_0 a constant, S_0 the SC area (cross section).

At each simulation time step the SCs were moved in the active area considering both the uniform sedimentation and the Brownian motion. The sedimentation motion of the SC carries on with a constant velocity, which is the consequence of the null resultant of three forces: gravity, Archimede's force and the viscous force in laminar flow regime (Stokes). Considering the SC with a spherical shape, the velocity is given by equation (3):

$$v_s=\frac{2r^2 g}{9\eta}\cdot\left(\rho-\rho_0\right) \tag{3}$$

where r is the radius of the sphere, ρ is the density of the scattering center, ρ_0 is the density of the fluid, η is the dynamic viscosity coefficient of the fluid. The fluid was considered to be water and the variation of the water density and dynamic viscosity with temperature was calculated by a polynomial fit on the experimental data in [15]. The sedimentation motion was modeled for each SC individually by changing the position with a distance equal with the v_s times the time step on the vertical direction. The time step for modeling the sedimentation motion is the inverse of the framerate, which is one of the input parameters. The framerate is actually the framerate used in calculating a movie or the sampling rate, of the data acquisition system used in recording a time series during a laboratory experiment.

The Brownian motion was modeled differently, though individually for each SC. The Maxwell – Boltzman velocity distribution is actually the product of the three velocity distribution function for one dimension:

$$f_v(v_i)=\sqrt{\frac{m}{2\pi kT}}\cdot\exp\left(-\frac{m{v^2}_i}{2kT}\right) \tag{4}$$

In (4) k is Boltzman's constant, T is the absolute temperature and m is the mass of the particle in thermal equilibrium with the environment and i can be either x, y or z. At each simulation time step the velocity values for v_x, v_y and v_z of each SC were therefore generated using random numbers with a normal distribution having the variance kT/m.

The Brownian motion time step is different of the sedimentation motion time step and was determined during another computer experiment that modeled the diffusion of the nanoparticles. The time step parameter was iteratively adjusted and the diffusion coefficient was calculated for each value. The Brownian motion time step was chosen to be the value that leads to a calculated D value equal to the Einstein theoretical value for the diffusion coefficient:

$$D=\frac{kT}{6\pi\eta r} \tag{5}$$

In order to find out which one of the two different type of motions, sedimentation and Brownian motion, has the bigger role causing the fluctuations of the scattered light intensity we notice that the mean square value of the velocity module, also called the thermal velocity, given by equation (6), is a measure of the Brownian motion intensity [16]:

$$v_t=\sqrt{\frac{3kT}{m}} \tag{6}$$

Figs. 2 and 3 present the variation of the sedimentation and of the Brownian motion velocities at 293K for particles having a diameter from 4 to 37 nm, hence a radius in the range 2 to 18.5 nm.

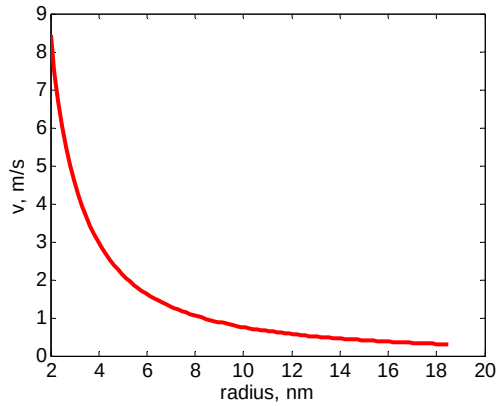

Fig. 2. The Brownian motion velocity versus particle radius in the range 0.2 – 18.5 nm at 293 K.

Examining Figs. 2 and 3 we notice that the sedimentation motion velocity is roughly 10^9 times smaller than the Brownian motion. This proves that for nanoparticles the Brownian motion is the main cause of the speckle fluctuations.

Beyond the constant phase change of the wavelets emitted by each SC, there does exist another major cause of the light intensity fluctuations in each location of the interference field, namely the variation of the number of SCs in the beam area.

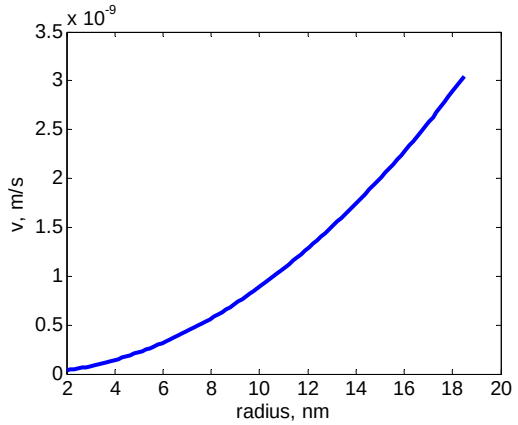

Fig. 3. The sedimentation motion velocity versus particle radius in the range 0.2 – 18.5 nm at 293 K.

As sedimentation goes on (less significant for nanoparticles but significant for micron size particles) some SCs fall below the lower edge of the beam area, therefore the contribution of the wavelets scattered by these SCs must be ignored. Other SCs fall down into the beam area and their contribution must be considered. These SCs number variations are considered by the program described in this paper and at the beginning of the computer experiment the SCs positions are generated in a volume that has the height:

$$h = h_0 + v_s \cdot t_{\exp} \tag{7}$$

where v_s is the sedimentation motion velocity, given by (3) and t_{exp} is the time span of the experiment.

Moreover, the Brownian motion is the major cause of the SCs number in the beam area fluctuation. This SC number variation was considered as well. At the beginning of the experiment both the initial volume the SC positions were generated into and the SC number were increased accordingly with the t_{exp} defined above, in order to have the desired average number of SCs in the beam volume of the cuvette.

For a realistic modeling only the contribution of the SCs located in the beam area at that moment was be added to compute the far field intensity, after moving each SC individually during each simulation step.

The program can be used to compute either an image of the far field, or a movie, with the desired frame rate and resolution, in a certain location of the far field, or the time series of the light intensity recorded by a detector with a certain dimension and location in the far field. Some results of the computer simulations are presented in the next section.

3. Simulation results

First the control parameters were adjusted to calculate a far field movie. A frame from the computed movie having 10 nm diameter nanoparticles as target is presented in Fig. 4.

The movie has the aspect of boiling speckles, exactly as a movie recorded during a laboratory light scattering experiment on diluted magnetic fluid.

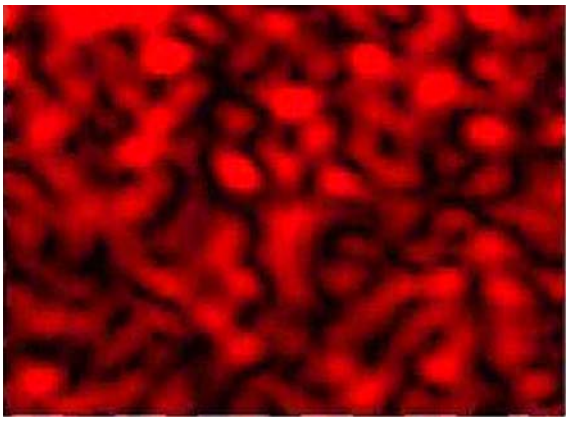

Fig. 4. A frame from the computed movie having 10 nm diameter nanoparticles as target.

Running the program with another value of the control parameter, a time series representing the far field intensity fluctuation was calculated. The cuvette-detector distance was 0.8 m, the detector was 0.005 m apart from the beam direction. A 0.1 second sequence of a time series recorded when the target consisted of 10 nm diameter nanoparticles is presented in Fig. 5.

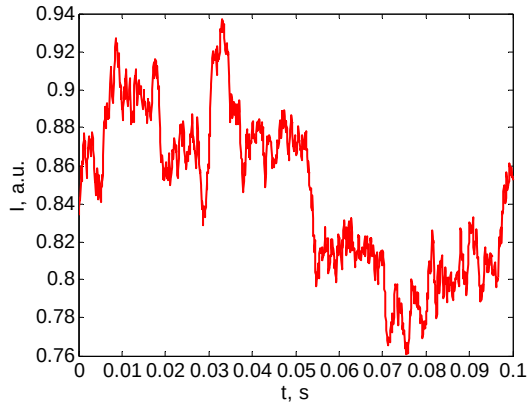

Fig. 5. A calculated time series for of 10 nm diameter nanoparticles.

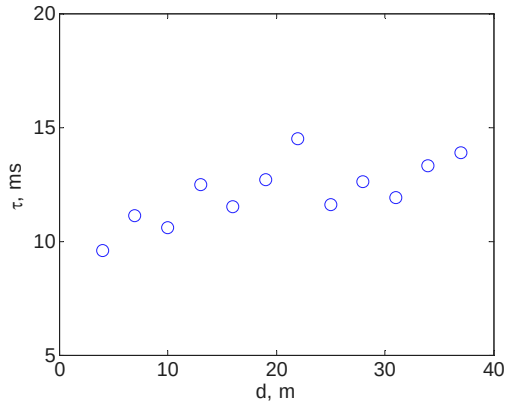

Fig. 6. The autocorrelation time variation with the SC diameter.

The autocorrelation function of each of the time series calculated with the program was calculated with (8) [17]:

$$A(\tau)=\frac{\langle E(\vec{r},t)*E(\vec{r},t+\tau)\rangle}{\langle E(\vec{r},t)*E(\vec{r},t)\rangle} \tag{8}$$

where the angle brackets denote averages over time t, r represents the position of the detector, and τ is the correlation time. The normalized autocorrelation function decreases from 1 and we can define the autocorrelation time τ as the time when the autocorrelation function decreases to 1/e.

When the fluid is flowing the SCs have a velocity v. The autocorrelation time has a variation with the particle in suspension velocity given by equation (9) [7], [8]:

$$\tau=\frac{A}{k\cdot v} \tag{9}$$

where k is the wave number and A is a constant depending on the scattering properties of the sample. The main idea in this paper is to calculate the autocorrelation time for nanoparticles of different sizes, that have both a uniform sedimentation motion and a chaotic, Brownian motion and to investigate the variation of the autocorrelation time with the particle size.

The program was run for particles with a diameter in the range 4 – 37 nm and produced time series for each target. The autocorrelation time was calculated for each target. The sampling rate of the assumed data acquisition system was 10000 per second. It is worth mentioning that the computer time required to produce a time series is very big, as the motion of each SC is individually calculated, growing linearly with the length of the time series and with the SC number.

The variation of the autocorrelation time with the SC diameter is presented in Fig. 5.

Examining Fig. 5 we notice that the calculated data has a relatively big spread. Nevertheless, an increase of the autocorrelation time with the size of the nanoparticles is obvious.

With the increase of the diameter the particle mass m increases and the velocity in (6) decreases. Consequently τ in (9), which was derived considering particles with velocities in one direction, decreases.

We found from this computer experiment that the autocorrelation time τ has same trend of decreasing with the increasing of the nanoparticle diameter although the velocity vector for nanoparticles is randomly oriented, rather than in one direction, as was considered when deriving (9).

4. Conclusions

The results of the computer simulation presented above were compared with the movie. The time series computed during the computer experiment were analyzed and the autocorrelation function was calculated and compared with the autocorrelation function of a time series recorded during a laboratory experiment performed on the real system with the same parameters. The computer simulation describes accurately both the far field interference aspect and the light scattering dynamics.

The computer simulation results presented in this work reveal that the autocorrelation time of a calculated time series decreases with the increase of the nanoparticle size. The nanoparticle size is one of the most important parameters that dictate the properties of a nanofluid or magnetic fluid. The results presented here suggest a low cost method of assessing the nanoparticle size, by recording a time series with a detector and a data acquisition system. First the time series are recorded and the autocorrelation time is calculated for magnetic fluids with known nanoparticle diameter. A calibration curve can be interpolated and used further on to assess the mean diameter of a magnetic fluid with unknown particles in suspension. If confirmed by accurate experimental results, the method proposed in this paper is much faster and has a

considerable lower cost than using an electron microscope or XRD. Experimental work is scheduled to verify the proposed method.

References

[1] U. S. Choi, ASME Fed. **231**, 99-103 (1995).
[2] P. Vadasz, J. Heat Transfer. **128**, 465-477 (2006).
[3] S. P. Jang, S. U. S. Choi, Appl. Phys. Lett. **84**, 4316-4318 (2004).
[4] W. Evans, J. Fish, P. Keblinski, Appl. Phys. Lett. **88**, 093116 (2006).
[5] Y. M. Xuan W. Roetzel, Int. J. Heat Mass Transfer. **43**, 3701-3707 (2000).
[6] R. Prasher, P. Brattacharya, P. E. Phelan, Phys. Rev. Lett. **94**, 025901 (2005).
[7] J. W. Goodman, in Laser speckle and related phenomena, Vol. 9 in series Topics in Applied Physics, J. C. Dainty, Ed., Springer-Verlag, Berlin, Heidelberg, New York, Tokyo, (1984).
[8] J David Briers, Physiol. Meas. **22**, R35–R66 (2001).
[9] W.-X. Fang, Z.-H. He(a), X.-Q. Xu, Z.-Q. Mao, H. Shen, European Physics Letters **77**, 68004-68009 (2007).
[10] Dan Chicea and Mihaela Răcuciu, J. Optoelectron. Adv. Mater. **9**(8), 2738 (2007).
[11] Ming Qian, Jun Liu, Ming-Sheng Yan, Zhong-Hua Shen, Jian Lu, Xiao-Wu Ni, Optics Express **14**(17), 7559 (2006).
[12] D. Chicea, M. L. Chicea, J. Optoelectron. Adv. Mater. **9**(3), 694 (2007).
[13] I. C. Kim, S. Torquato, J. Appl. Phys. **69**, 2280 (1991).
[14] M. Hammer, A. N. Yaroslavsky, D. Schweitzer, Physics in Medicine and Biology", **46**, N65-69 (2001).
[15] http://www.thermexcel.com/english/index.htm
[16] I. C. Kim, S. Torquato, J. Appl. Phys. **69**, 2280 (1991).
[17] R. Bracewell, The Fourier Transform and Its Applications, 3rd ed. New York: McGraw-Hill, 40-45 (1999).

*Corresponding author: dan.chicea@ulbsibiu.ro